Applied Catalysis B: Environmental 117–118 (2012) 302–309

Contents lists available at SciVerse ScienceDirect

Applied Catalysis B: Environmental

journal homepage: www.elsevier.com/locate/apcatb

Single-stage medium temperature water-gas shift reaction over Pt/ZrO_2 – Support structural polymorphism and catalyst deactivation

Carlos A. Franchini, Andréa M. Duarte de Farias, Elise M. Albuquerque, Renata dos Santos, Marco A. Fraga *

Instituto Nacional de Tecnologia/MCT, Laboratório de Catálise, Av. Venezuela, 82/518, 20081-312 Rio de Janeiro, Brazil

ARTICLE INFO

Article history:
Received 16 October 2011
Received in revised form 11 January 2012
Accepted 24 January 2012
Available online 1 February 2012

Keywords:
Deactivation
Polymorphism
Zirconia
Monoclinic
Tetragonal
Fuel cell

ABSTRACT

Influence of zirconia polymorphism on water-gas shift reaction was investigated. The study was carried out over catalysts with similar features, which allowed assessing any effect brought about by the support crystalline structure. It was found that zirconia polymorphism determines the catalyst activity and the monoclinic structure renders a more active system. It is most likely due to the presence of hydroxyl groups, which have been claimed to be involved in the formation of important reaction intermediates. Catalyst deactivation was also addressed and it could be concluded that the changes in metal phase dispersion along reaction play a quite important role on the ZrO_2-supported catalyst stability.

1. Introduction

The water-gas shift reaction (WGS) involves the conversion of CO to CO_2 while generating hydrogen. It makes possible the increase of hydrogen concentration and the minimization of CO concentration, adjusting thus the H_2/CO ratio in reformate streams for industrial processes. Due to conversion constraints imposed by chemical equilibrium, it is traditionally a two-step process with a high temperature (HTS) stage at 350–500 °C, followed by a low temperature (LTS) stage at 200–250 °C. The chemical characteristics of the reaction have been driving a growing interest especially due to its potential application in fuel cell technology. However, the commercially available catalysts for this two-step process do not fit the requirements for hydrogen production in a fuel processor. The usually large volumes required for the shift reactors, which are responsible for about 50% of the total volume of the fuel processor [1], may be outlined as one of the meaningful barriers for cost-effective small size fuel processor systems.

Undoubtedly, the catalyst is a crucial point of this chemical transformation and, although new formulations have been studied along the past decades, an increase in the catalytic activity is still desired aiming to address economical issues. One feasible approach must involve the merging of the two steps of the reaction process resulting preferably in a unique medium temperature water-gas shift stage. Noble metal based catalysts have been shown to be promising systems to accomplish such goal [2–4] and thus expand WGS application in the energy power generation systems. The development of new catalytic formulations to fit those requirements also gave rise to the study of a vast list of oxides as supports [5]. Their structural and superficial characteristics have been receiving considerable attention when studying the catalyst design [6–9]. For example, the presence of OH groups, oxygen vacancies, structural defects and support reducibility are some points that commonly come up when discussing the catalysis for WGS reaction [2,5,10]. These points have become key factors in the researchers' efforts to understand the reaction mechanism. These mechanisms are proposed to be either redox [11] or formate [12] mediated routes.

The redox mechanism, also known as regenerative mechanism, is based on the adsorption of CO on metallic sites. These species are responsible for reducing the support releasing CO_2. The partially reduced support is reoxidized by the adsorption and dissociation of water. As for the formate route, also known as associative mechanism, intermediate formate species are generated from the reaction of adsorbed CO with OH surface groups; these species finally decompose into CO_2 and hydrogen in the presence of water. A third suggestion, a hybrid mechanism derived from a combination of those previous two, has also been proposed [13]. As a matter of fact, a thought-provoking discussion has been openly presented

* Corresponding author. Tel.: +55 21 21231152; fax: +55 21 21231166.
E-mail addresses: marco.fraga@int.gov.br, fraga_marco@yahoo.com.br (M.A. Fraga).

0926-3373/$ – see front matter © 2012 Elsevier B.V. All rights reserved.
doi:10.1016/j.apcatb.2012.01.028

in the literature concerning different evidences to support these current approaches.

Zirconium oxide has been investigated on WGS and a promising performance is frequently mentioned [13–15]. Considering the low reducibility [16] and the consequent low oxygen storage capacity of this oxide [17] it would thus be quite unlikely that the redox mechanism could proceed over ZrO_2-supported systems. Nevertheless, some results published elsewhere [13] have showed that zirconia support may provide oxygen under WGS conditions even if surface hydroxyl groups have been depleted. On the other hand, as expected for any oxide [18], zirconia surface is populated with hydroxyl groups, which, in the right configuration, could also play a role on the generation of formate species promoting WGS through the associative mechanism [13,19]. As either route is conceivable and experimental evidences have been successfully provided, the hybrid mechanism – 'associative mechanism with redox regeneration' – has been claimed to be a valid hypothesis for ZrO_2-supported catalysts [13].

This literature background has encouraged some studies on different polymorphic phases of ZrO_2 support [20–22] since it is recognized that the coordination environment of zirconium and oxygen in the oxide varies as a function of the structure [23]. Nevertheless, some controversial conclusions have been reached as the monoclinic phase was found to be a more effective support for gold [22] while tetragonal ZrO_2 has been reported as highly active for copper catalysts [21]. It is interesting to note that both studies have considered the associative mechanism. On one hand, the production of formate species was claimed to be favored by the surface hydroxyls on monoclinic zirconia, rendering an active catalyst [22]. On the other hand, a negligible activity on the same polymorphic structure was ascribed to the high stability of the exactly same intermediate surface species by other groups [21].

As for platinum-based catalysts, only one contribution regarding ZrO_2 structural polymorphism can be found in the literature [20]. Based on *in situ* infrared spectroscopic results, Chenu et al. predicted that monoclinic phase-supported catalyst would be more active for WGS by ranking the intensities of formate vibration bands generated after CO adsorption on the reduced samples [20]. Such prediction could be indeed corroborated by the catalytic activity measurements.

To scrutinize these apparent conflicting results, it should be taken into account that all these studies conducted over zirconia polymorphs were carried out over catalysts with different metal phase, at low [22] or medium [21] temperature and under a mixture containing only CO and water. It is well known that CO_2 and hydrogen, produced during the preceding reforming stage of the fuel processor, hinder the WGS equilibrium reaction [24,25] and thus their role must be well thought-out from the perspective of catalyst design and engineering.

Deactivation is also an important issue to be considered if the designed catalyst is meant to be used in industrial applications. Some recent papers have been dealing with this matter but they are mostly focused on catalysts supported on reducible oxides [2,13,26–29]. A systematic study attempting to identify any effect from structural polymorphism on deactivation is still missing.

Therefore, in this work the influence of zirconia polymorphism on WGS catalyzed by platinum-based systems is methodically investigated. The experiments were carried out over catalysts with similar characteristics in order to unambiguously assess any effect brought about by the crystalline structure of the support. Moreover, it aims at further contributing to the understanding of the deactivation process undergone by the supported WGS noble metal catalysts. In this approach, the presence of both H_2 and CO_2 along with the WGS typical feed compounds (H_2O and CO) was taken into account over all catalytic evaluation.

2. Experimental

2.1. Sample preparation

Monoclinic and tetragonal zirconias were supplied by Norpro and used as supports for the preparation of Pt-based systems. The catalysts were prepared by incipient wetness impregnation with an appropriate volume of a $(NH_3)_4Pt(NO_3)_2$ (99% from Acros) aqueous solution to obtain 1% (wt.) Pt in the final composition. Impregnated samples were dried at 120 °C for 16 h and calcinated under air at 500 °C for 4 h.

2.2. Sample characterization

Powder XRD patterns were recorded on a Rigaku Miniflex diffractometer that uses Cu Kα radiation operated at 30 kV and 15 mA. The samples were spread as thin layers on a glass slide and diffraction patterns were obtained by increasing 2θ with 0.02° steps in the range 10–80°.

Surface areas were determined from the adsorption isotherms through the BET method. The N_2 adsorption experiments at −196 °C were carried out on an ASAP 2020 from Micromeritics. The materials were previously submitted to a pre-treatment being outgassed at 5 mm Hg and 150 °C for 24 h.

The supports were also investigated by Fourier transform infrared spectroscopy (FTIR). Self-supported wafers were pretreated under vacuum at 500 °C for 1 h, submitted to an air flow at the same temperature for 30 min and then finally evacuated for more 30 min. The sample was cooled down to room temperature and the spectra collected with 256 scans and resolution of 4 cm^{-1} in a Nicolet Magna 560 spectrometer.

Total acidity of the supports was determined by *n*-butylamine adsorption. The supports were treated at 500 °C under N_2 for 30 min; next, the temperature was decreased to 150 °C and then the samples were exposed to *n*-butylamine for 30 min to saturate the acid sites. To remove the physisorbed base, the supports were flushed with N_2 for 30 min. Finally, samples were submitted to thermogravimetric analysis in a TA Instruments SDT Q600, with a heating rate of 20 °C min^{-1}, up to 800 °C under N_2 (100 mL min^{-1}).

The chemical composition of all catalysts was determined by X ray fluorescence analyses, which were carried out on a Shimadzu EDX-700 spectrometer.

Temperature-programmed desorption of CO (TPD-CO) was carried out in a flow reactor attached on-line to a quadrupole mass spectrometer Ominstar Balzers QMS200. Initially, the catalyst was reduced *in situ* at 350 °C for 1 h under pure hydrogen. Afterwards, the gas was switched to helium, heated up to 500 °C and finally cooled down to room temperature. CO was admitted into the reactor and the adsorption was allowed to proceed for 30 min. After purging the reactor, the temperature was raised up to 500 °C under helium and the eluting gases were monitored.

Temperature-programmed surface reaction (TPSR) was also carried out in the same equipment described previously for the TPD-CO analyses. The exactly same steps were followed prior to analyses, but the desorption was carried out under a flow of helium with 30% of water, which was accomplished by using a saturator.

Dispersion of both fresh catalysts was determined by hydrogen chemisorption performed at 35 °C in a Micromeritics ASAP 2010 equipment. Before analysis, the samples were submitted to an *in situ* reduction treatment under hydrogen at 350 °C for 1 h. Platinum dispersion was calculated by assuming a stoichiometry (H:Pt) of 1:1 [30].

The reaction rate of cyclohexane dehydrogenation was used to estimate the apparent metallic dispersion of the spent catalysts [31,32]. The experiments were carried out according to a detailed protocol described elsewhere [2]. Briefly, the catalysts

were dried under N_2 at 150 °C for 30 min and then reduced at 350 °C (10 °C min^{-1}) for 1 h under pure hydrogen before admitting a mixture of cyclohexane in hydrogen into the reactor. A H_2/C_6H_{12} ratio of 13.2 was used in order to avoid the catalyst deactivation due to carbon deposition [33]. The reaction rates were calculated under differential conditions at 260 °C and the C_6H_{12} conversion was determined as an average of multiple and consecutive gas chromatography analyses. No deactivation was observed during these experiments. The reaction products were monitored by on-line gas chromatograph (Agilent 6890N) equipped with a FID detector. Dispersion was determined by analyzing the fresh catalysts as well and correlating their reaction rates with those values previously obtained by hydrogen chemisorption. It is important to mention that a satisfactorily linear correlation between the rate of cyclohexane dehydrogenation and platinum dispersion as measured by hydrogen chemisorption was obtained.

Temperature-programmed oxidation (TPO) analyses were performed with the spent catalysts in order to estimate the total amount of carbonate complexes formed along 20 h WGS reaction. The experiments were carried out in a thermobalance SDT Q600 from TA Instruments under synthetic air (20% O_2/N_2) at 50 mL min^{-1} and the temperature was increased linearly at a rate of 20 °C min^{-1} up to 600 °C.

The spent catalysts were also examined by Fourier transform infrared spectroscopy (FTIR). The spectra were collected by using a thin wafer of the spent catalyst (3 wt.%) in KBr. 32 scans with resolution of 4 cm^{-1} were registered in a Nicolet Magna 560 spectrometer.

2.3. Catalytic evaluation

Catalytic stability tests were performed in a U-shaped fixed-bed flow reactor. To reproduce typical conditions of the outlet of an ethanol fuel reformer [34], a gas mixture with a composition of 5.49% CO, 4.10% CO_2, 9.71% H_2, 30.75% H_2O (H_2O:CO molar ratio = 5.6:1) and N_2 (balance) was used. Water was added into the gas stream by using a saturator at 70 °C. The WGS was performed at 300 °C with 120 mg of catalyst diluted in SiC (1:5) in order to avoid temperature gradients in the reactor, and a total gas flow of 90 mL min^{-1}. Before reaction, the catalysts were reduced in H_2 (30 mL min^{-1}) from room temperature to 350 °C (10 °C min^{-1}) for 1 h. Subsequently, the system was purged with N_2 (30 mL min^{-1}) while the temperature was lowered to 300 °C. The reformate gas mixture was then admitted into the catalyst bed and the reaction was monitored for 20 h. The reactor effluent was analyzed on-line with a gas chromatograph (Agilent 6890N) equipped with a TCD detector, providing CO, CO_2 and H_2 concentrations.

3. Results and discussion

3.1. Sample characterization

The XRD analyses of the commercial supports are depicted in Fig. 1. XRD patterns were identified by comparison with JCPS files 37-1484 and 42-1164 and confirmed that they consist of monoclinic (*m*-ZrO_2) and tetragonal (*t*-ZrO_2) zirconia phases. Line broadening analysis of the peaks associated with (−1 1 1) and (1 1 1) reflexions for *t*- and *m*-ZrO_2, respectively, was conducted applying Scherrer equation. The resulting crystallite diameters of the two samples are virtually the same (Table 1). Accordingly, N_2 adsorption analyses indicated that both materials have high surface area (S_{BET}), with the tetragonal sample exhibiting a slightly higher value as shown in Table 1.

As the crystalline phases have been positively identified as two different zirconia polymorphs, one can expect a variation in the catalytic performance due to the differences in the short range order around O and Zr atoms. Indeed, in the tetragonal lattice the Zr^{4+} cation is octacoordinated and the O^{2-} anion is tetracoordinated, whereas in the monoclinic lattice the Zr^{4+} cation is heptacoordinated and the O^{2-} anion is either tri- or tetracoordinated [23]. The hydroxylation of the oxide surface is also affected by the difference in the structural organization. Distinct concentration and type of hydroxyl groups are formed to coordinate the surface atoms. At the same time, the density of potential coordinatively unsaturated sites (CUS) on their preferential planes should also be expected to be distinct, as already determined by Zhao et al. [23]. Another interesting aspect comes from the co-existence of basic and acid surface structures which would render its denomination as amphoteric oxide. In view of these findings, it is likely that the structural characteristics of each crystal form will reflect in their interaction with reactants and hence a close analysis of such features was systematically carried out.

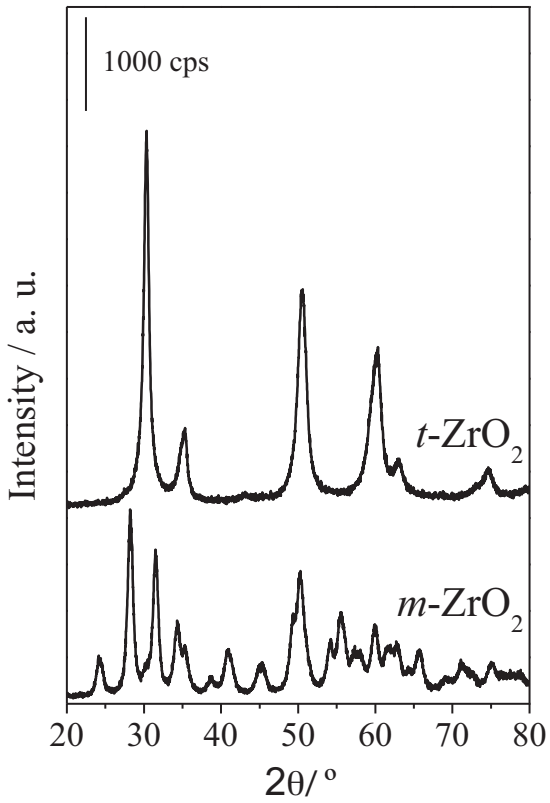

Fig. 1. X-ray diffraction patterns of the commercial zirconia polymorphs.

Infrared spectra were collected after partial dehydroxylation at 500 °C under vacuum aiming at gathering information about the polymorphs surface functional groups. The spectra revealed that *m*-ZrO_2 and *t*-ZrO_2 possess different terminal hydroxyl surface groups as observed previously by Jung and Bell [35]. By analyzing the O—H stretching region displayed in Fig. 2, two well-defined narrow vibration bands at 3772 and 3673 cm^{-1} were observed for *m*-ZrO_2,

Table 1
Surface area (S_{BET}), crystallite mean particle size (d_{hkl}) and density of acid sites of the catalysts.

Support	S_{BET} (m^2/g)	d_{hkl} (nm)	Density of acid sites (μmol *n*-butylamine/m^2)
m-ZrO_2	94	10.1[a]	5.17
t-ZrO_2	121	10.5[b]	3.93

[a] Line broadening analysis of the peak associated with (1 1 1) reflexion.
[b] Line broadening analysis of the peak associated with (−1 1 1) reflexion.

Table 2
Chemical composition, Pt dispersion, reaction rate and CO_2 desorbed from the catalysts.

Catalyst	Pt (wt.%)	Dispersion (%)	Reaction rate[a] (mmol C_6H_{12}/g_{cat} h)	Ea[b] (kJ/mol)	Reaction rate[c] (μmol CO/g_{Pt} h)	CO_2[d] (μmol CO_2/g)
Pt/*m*-ZrO_2	1.10	30	163.6	101	9.56	141
Pt/*t*-ZrO_2	0.98	25	118.8	125	6.39	193

[a] Reaction rate refers to the dehydrogenation of cyclohexane at 260 °C.
[b] Apparent activation energy of the dehydrogenation of cyclohexane.
[c] Reaction rate refers to the WGS reaction at 300 °C.
[d] CO_2 desorbed from the used catalysts as determined by TPO.

indicating isolated OH groups. These findings are consistent with the monoclinic structure and can be attributed to mono and multi-coordinated OH [19,36,37], respectively. On the other hand, no signal of mono-coordinated hydroxyl groups could be seen in the OH-vibrational spectra of tetragonal-based sample. An ill-defined broad absorption roughly centered at 3650 cm^{-1} was registered, indicating the establishment of strong hydrogen-bonding, possibly between bulk species [15,38].

The acid–base relation on the surface of zirconia polymorphs is determined by the presence of OH groups (Bronsted acidity), as previously described herein, or coordinated unsaturated Zr^{4+} cations (Lewis acidity) [39]. In order to probe these unsaturated sites, adsorption/desorption of *n*-butylamine was carried out and quantitatively assessed by thermogravimetry. As regarding the adsorption of this amine, it may be considered that one mol of chemisorbed *n*-butylamine corresponds to one mol of acidic sites [40]. The data calculated from the thermal analyses is also summarized in Table 1 as normalized by BET surface areas. It can be seen that the tetragonal zirconia possesses lower number of coordinatively unsaturated sites, suggesting that such polymorphic structure is characterized by lower density of structural defect sites such as steps, corners and typical defective positions. A dependence between surface features and structural/morphological characteristics has been evidenced for some other oxides with a consequent distribution of acid–base sites [41]. This result suggests that under WGS atmosphere, the higher concentration of coordinatively unsaturated sites on the monoclinic structure would allow a more extensive adsorption of CO molecules on the support due to their weak basic nature. Consequently, the catalytic activity could be favored if the associative mechanism is taken into consideration.

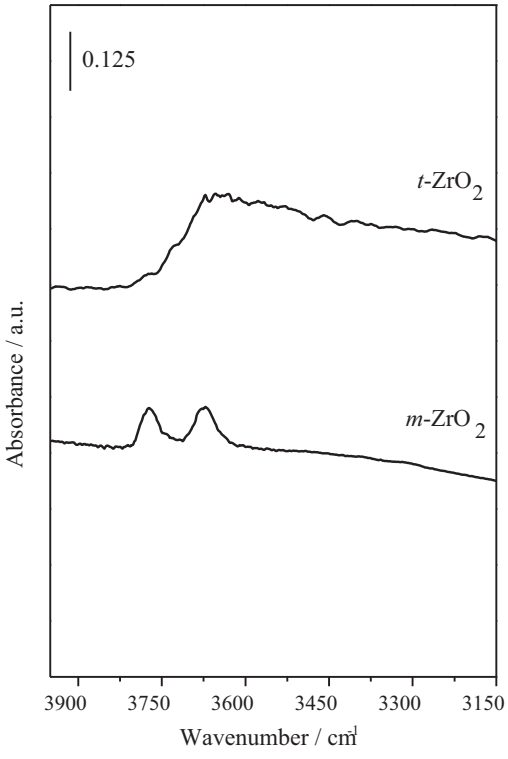

Fig. 2. OH region of infrared spectra of the commercial zirconia polymorphs.

The role played by platinum metallic sites in WGS reaction cannot be disregarded since Pt—CO bonds will also be certainly established. Therefore, metal loading and dispersion of both catalysts were determined. As presented in Table 2, the catalysts possess fairly similar metal content, which satisfactorily meets the nominal composition. Likewise, metal dispersion as measured by hydrogen chemisorption allows a straightforward examination of any possible influence from the support polymorphism on the catalyst performance on WGS.

Temperature-programmed desorption experiments were conducted to investigate the interaction of CO with the polymorphic catalysts. Fig. 3 shows the thermodesorption patterns of the catalysts after being exposed to CO. In both cases, CO desorption is negligible and the main detectable compounds are CO_2 and hydrogen, indicating that CO molecular desorption from the catalyst surface almost does not occur but a surface reaction is promoted instead. Therefore, the amount of both CO and CO_2 in the desorption profiles should be taken as an estimative of the total amount of primarily adsorbed CO. The results depicted in Fig. 3(a and b) are indeed in line with the behavior revealed previously from the adsorption of *n*-butylamine, which predicted a higher adsorption capacity of CO for the monoclinic polymorphic oxide. Furthermore, the registered profiles clearly point toward the occurrence of WGS reaction even in the absence of water, as reported elsewhere [9,19].

With the purpose of differentiating and examining the distinct contributions of both hydrogen and CO_2, these profiles were deconvoluted by considering a multiple-Gaussian function for fitting the experimental curves. Several mathematical contributions were required to fit the experimental patterns. The numerical calculations were executed with a nonlinear routine to minimize the square of the deviations and the position of each peak was taken as an initial estimate. This mathematical routine was shown to adequately fit the experimental data as presented in Fig. 3. All components are depicted in dotted lines and designated by numbers.

The H_2/CO_2 ratios experimentally determined for both samples are summarized in Table 3. Both compounds were detected for Pt/*m*-ZrO_2 and a ratio close to the expected theoretical value of 1 was obtained (Fig. 3a, peaks 1–4), suggesting that the surface hydroxyl groups from *m*-ZrO_2 may likely react with the adsorbed CO. A slighlty higher value for H_2/CO_2 ratio was accomplished at above ~450 °C (Fig. 3a, peak 5). It is most likely credited to the desorption of hydrogen strongly chemisorbed or spiltover, whose

Table 3
Experimental H_2/CO_2 ratio as determined by TPD-CO.

Catalyst	H_2/CO_2				
	1	2	3	4	5
Pt/*m*-ZrO_2	0.95	0.98	0.98	0.73	1.17
Pt/*t*-ZrO_2	–	0.94	0.88	0.70	–

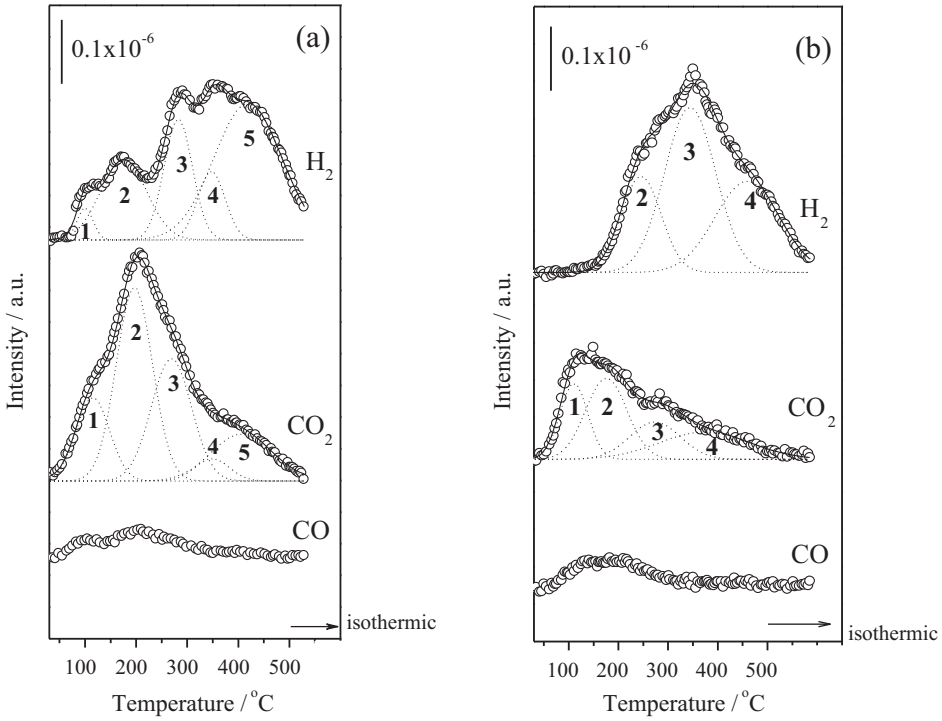

Fig. 3. TPD-CO profiles of both studied catalysts: (a) Pt/*m*-ZrO_2, and (b) Pt/*t*-ZrO_2.

adsorption occurs upon the early reduction stage needed for catalyst activation. It has indeed been observed by other groups [42].

Analyzing the TPD curves obtained for Pt/*t*-ZrO_2 (Fig. 3b), it can be seen that only CO_2 is detected at around 100 °C (peak 1) along with a timid desorption of CO. Formation of hydrogen was not registered at this low temperature range. Contrasting with the monoclinic polymorph-supported catalyst, it could be envisaged that no WGS reaction occurs over this sample at this point. Instead, the production of CO_2 may happen through CO oxidation with zirconia surface providing the oxygen [43] or through the disproportionation of CO according to Boudouard reaction [42,44]. The concomitant CO_2 and hydrogen evolution observed from 200 °C is an indicative that WGS is then occurring. Indeed, an equivalent release of these compounds may be discriminated by deconvoluting their profiles (Fig. 3b, peaks 2–4; Table 3). This result suggests that the tetragonal structure would render a less active catalyst for WGS.

Control experiments with both pure supports were also performed in order to address the role of Pt metallic sites and the polymorphs. No signals of hydrogen, CO or CO_2 were detected, indicating that no WGS reaction takes place over the platinum-free polymorphs. Indeed, the results from the control experiments are in line with the previous spectroscopic study carried out by Graf et al. [19]. Even though the interaction between CO and hydroxyl groups on zirconia has been evidenced to occur in the absence of Pt by different authors [45,46], Graf et al. [19] showed that the surface species generated on Pt-free samples are reversible and do not decompose into gaseous products. The hydroxyl groups on zirconia are recovered as soon as CO is removed from the stream. WGS gaseous products (CO_2 and H_2) can only be formed when platinum was present in the catalyst [19,42]. The results presented in this work corroborate such findings and restated the crucial role played by the metallic sites in generating the gaseous products during reaction. Furthermore, they evidence the importance of the superficial arrangement of the zirconia support when dealing with WGS. The monoclinic support demonstrates a better interaction with CO molecules due to the configuration of OH groups located on the surface as well as a higher concentration of coordinatively unsaturated sites. Indeed, it is interesting to mention some published studies [19,20] where OH reactivity is directly correlated to WGS activity. Here, the principal aspect is the participation of terminal and bridged hydroxyl groups of the monoclinic structure, also named as mono and multi-coordinated hydroxyls, respectively. Terminal OH groups are considered to react with CO to produce formate species and their decomposition follows with the aid of Pt particles and the bridged OH [10,19,42].

TPSR experiments were also conducted on both catalysts. In these trials, the samples were also exposed to the thermal treatment after reduction in order to diminish the concentration of any chemisorbed hydrogen as previously carried out for the TPD analyses. Only after reaching back the room temperature and performing CO adsorption, water vapor was added to the stream while the temperature was raised. The resulting patterns are shown in Fig. 4 where the same set of molecules produced during TPD-CO can be observed. The key difference between TPD and TPSR analyses stems from the simultaneity of the first peak for CO_2 and H_2. The parallel production of these compounds is interpreted as the onset of WGS reaction as the essential reactants are present on the catalyst surface during TPSR experiments. It is also important to note that the evolution of the reaction products occurs at lower temperature for Pt/*m*-ZrO_2 (Fig. 4a), around 50 °C below that registered for Pt/*t*-ZrO_2 (Fig. 4b). This result would also evidence a higher catalytic activity for monoclinic-supported sample, as predicted so far by the probed chemical features of the catalytic systems reported herein. It is worth mentioning that, similarly to what was observed in the TPD analyses, no gaseous products were detected in the control experiments carried out with both pure zirconia polymorphs.

3.2. Catalytic evaluation

The WGS overall activities were evaluated based on the CO conversion, revealing that the catalysts behave quite differently (Fig. 5). As expected from the characterization analyses presented before, the Pt/*m*-ZrO_2 sample showed to be markedly more active,

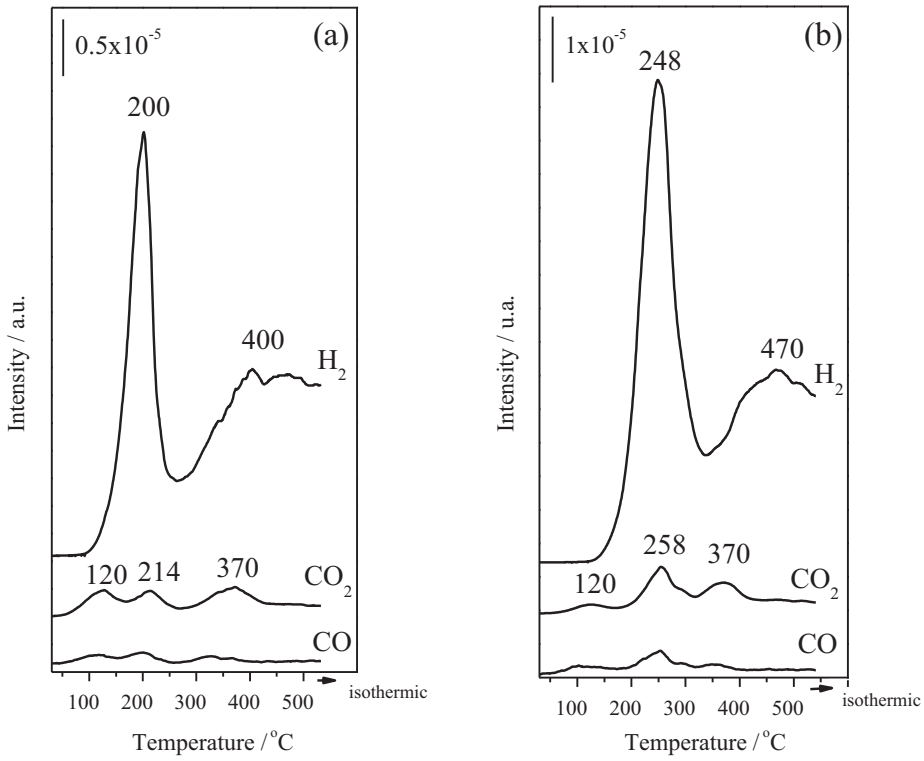

Fig. 4. TPSR profiles of both studied catalysts: (a) Pt/*m*-ZrO_2, and (b) Pt/*t*-ZrO_2.

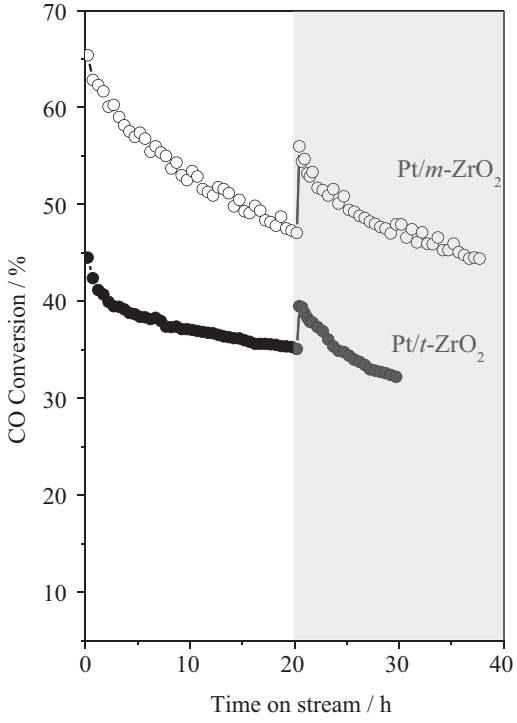

Fig. 5. CO conversion at 300 °C as a function of time on stream (5.49% CO, 4.10%CO2, 9.71% H_2, 30.75% H_2O) before and after (shadowed area) reactivation with air at 500 °C for 1 h.

reaching a conversion level 45% higher than that accomplished with Pt/*t*-ZrO_2. The initial reaction rates were also calculated by using a differential reactor (Table 2) and confirm this result. Basically, it might be associated with the presence of bridged hydroxyl groups on the oxide surface, mentioned above, which have been claimed to be the active sites for this reaction [10].

It is important to stress that these activity data were collected under a reformate composition containing both CO_2 and H_2, mimicking an actual reformate stream. It has been shown that the inhibiting effect of both gases is critical for the catalyst performance [3,24,25] and thus the use of simple mixtures containing only CO and water should be strongly discouraged.

The stability of the catalysts was analyzed by running a 20-h long experiment, generating a CO conversion profile as a function of time on stream (Fig. 5). A gradual decrease in activity was recorded for both samples; however, diverse catalyst deactivation kinetics is seen for these systems, with a particular and noticeable deeper drop of activity shown by Pt/*m*-ZrO_2 after the same period of time. It was also observed that the outstanding difference in their catalytic performance was maintained over the whole experiment. At this point, in the case of zirconia, it is possible to argue that the crystallographic arrangement of the support has a significant influence in the global and intrinsic activity in the course of WGS.

The deactivation process of WGS catalysts is still generally underestimated by authors and only few reports dedicated to the identification of the causes for the activity loss can be found. From the studies published so far, some tentative explanations can be highlighted. Deactivation of catalysts prepared over reducible supports is either associated with strong-metal support interaction (SMSI) established during the reduction step [13] or with the support reduction itself [28]. In the first case, the adsorption of hydrogen and/or CO on catalyst surface is hindered with a consequent reaction inhibition [13]. As for the support overreduction, it would lead to a loss of surface area, which would also affect WGS reaction [28]. Either way, the deactivation process may be reversed through an oxidation treatment.

Generation of stable carbonates species [26,27,29] on the catalyst surface and the sintering of metal particles upon WGS reaction

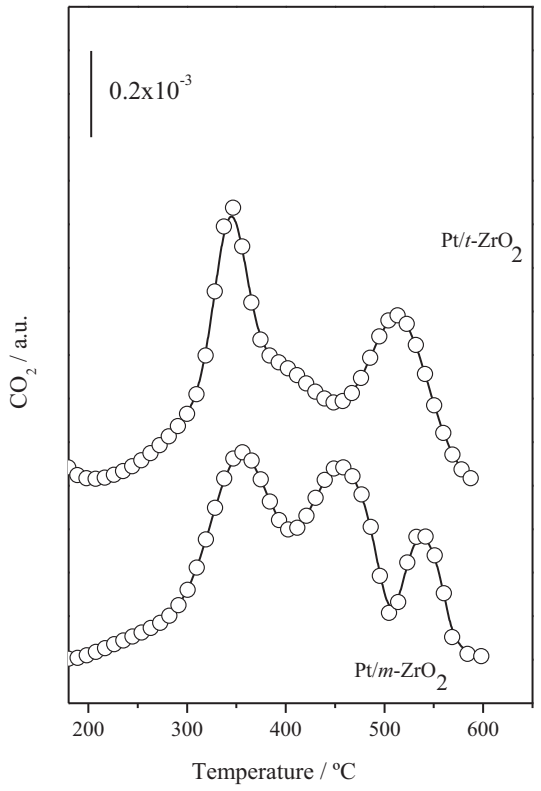

Fig. 6. TPO profiles of all spent catalysts. Analysis conditions: 20% O_2/N_2 at 50 mL min^{-1}, temperature was increased up to 600° (20° min^{-1}).

conditions have also been claimed as responsible for activity loss. As for platinum-based catalysts, Azzam et al. [13] supposed that under WGS environment the *in situ* production of formaldehyde could be responsible for the increase in the mobility of Pt particles, which would eventually lead to sintering. The authors considered that these oxygenate molecules are generated by the catalyst exposure to CO/H_2 and, in a minor extent, water vapor. A combination of all these phenomena has also been pointed as the main cause for the deactivation observed on catalysts supported on ceria-zirconia [29]. Recently, a highly active Ce–Sn–Pt catalyst has been presented and proven to be stable for WGS reaction under a reactant mixture simulating a reformate outlet and neither sintering nor carbonate deposition were observed whatsoever [47]. In this case, the authors claimed that the high dispersion achieved for Pt particle upon synthesis and their interaction with Sn were capable of avoiding sintering.

Considering the present scenario and the chemical nature of the catalysts used in this work, the establishment of SMSI or support overreduction is quite doubtful. Furthermore the formation of carbonate on the catalyst surface seems also to be a questionable explanation. Even though it has been shown to play a role in the case of ceria-containing systems, the likelihood of zirconia poisoning by carbonate species seems far lower since such species are unstable on ZrO_2 at around 300 °C [9,48]. All in all, the possibility of active sites blockage by other carbon-based species could not be ruled out in this case though. Hence the attempts to describe and understand the deactivation process observed for the two polymorphic samples presented herein focused on the formation of such carbon-based surface species and metal sintering.

Initially, the spent catalysts (after 20-h reaction run) were submitted to TPO experiments to shed some light on any contribution from carbon-based species to the catalyst deactivation under WGS conditions (Fig. 6). The registered profiles of CO_2 evolution presented broad peaks at above 300 °C, evidencing the occurrence of carbon-containing complexes on the catalyst surface. The infrared spectra of the spent catalysts were collected in an attempt to infer on the nature of such surface complexes but the spectral resolution was quite poor to provide any reliable evidence. It is probably due to the use of SiC as diluent for the reaction experiments. Although the molecular structure of such species could not be determined in this work, formate, carbonyl and formaldehyde-based deposits are plausible surface species to be considered as pointed out elsewhere [13].

The total amount of CO_2 released from the used samples is summarized in Table 2. It is seen that the slightly lower concentration of carbon-based complexes formed on Pt/*m*-ZrO_2 is incongruent with the pronounced difference on deactivation rate shown in Fig. 5. Therefore, it seems at first that catalyst deactivation is not straightly related to the concentration of such surface species.

In order to provide supplementary evidence to support this suggestion, the catalysts were submitted to a thermal treatment under an oxidant atmosphere (air) at 500 °C for 1 h right after the 20-h reaction run. They were then cooled down to 300 °C and the WGS reaction mixture was admitted into the reactor. From this point on, WGS reaction was monitored again for more 10–15 h (time-on-stream). This thermal treatment procedure would be able to decompose any carbon-based complex as revealed by the TPO profiles (Fig. 6), leaving a clean active surface and, consequently, should permit the thorough activity recovery. Along with the initial behavior of the fresh catalysts, Fig. 5 contrasts the catalytic performance after the exposition to such reactivation treatment (shadowed area). It is seen that over Pt/*t*-ZrO_2 the initial CO conversion level was 45%, dropped to 35% after 20-h reaction, reached 40% just after the thermal treatment and rapidly dropped back to 35%. A similar pattern was drawn for Pt/*m*-ZrO_2 that started at 65% conversion, decreased to around 48% after the first cycle (20 h), reached a conversion of 56% after reactivation treatment but returned to 47% after around 10 h. These experiments clearly showed that, especially for Pt/*m*-ZrO_2, the initial activity can only be partially and briefly recovered by cleaning up the catalyst surface through the decomposition of carbon-containing complexes. It is therefore possible to argue that the formation of carbon-based species upon WGS reaction does not play a major role in deactivation, if any.

A second attempt to understand the deactivation process involved the analysis of metal dispersion of the spent catalysts. It is not an ordinary task since the catalyst must be diluted with SiC (catalyst:SiC 1:5) with the aim of avoiding any temperature gradient in the catalytic bed due to the reaction exothermicity. With such approach, the examination of platinum dispersion by hydrogen chemisorption, as formerly done for the fresh samples, is not possible at all. Therefore, the metal dispersion after WGS reaction was estimated by calculating the rate of cyclohexane dehydrogenation. This reaction is known to be structure-insensitive and has been successfully used for this purpose whenever the catalytic system does not allow a direct analysis by conventional techniques [2,31]. A straight correlation between the cycloalkane dehydrogenation rate and the dispersion obtained from more traditional methods (chemisorption and transmission electron microscopy) is often established [32]. Indeed, the results obtained in the present work for the fresh catalysts from both cyclohexane dehydrogenation and hydrogen chemisorption (Table 2) are extremely consistent and allow a satisfactory assessment of platinum dispersion for the spent samples. Moreover, the apparent activation energy obtained for these catalysts (Table 2) is fairly constant and rather similar to those usually reported for platinum-based catalysts in the literature [31], which certify such method to determine metal dispersion [31].

In order to trail any change in dispersion along reaction, both polymorphic catalysts were analysed at three different stages – right after activation (fresh catalyst), after the first 20-h period under WGS environment (spent catalyst) and at the end of the

Table 4
Reaction rate of cyclohexane dehydrogenation of the spent catalysts.

Catalyst	Reaction rate[a] (mmol C_6H_{12}/g_{cat} h)		
	Fresh	After 20-h run	After second cycle
Pt/*m*-ZrO_2	163.6	85.6	61.2
Pt/*t*-ZrO_2	118.8	87.8	77.1

[a] Reaction rate calculated at 260 °C.

second cycle of WGS reaction which followed the reactivation procedure. The results shown in Table 4 disclose a gradual drop in platinum dispersion for both catalysts. Interestingly, a stronger decrease in dispersion (~50%) was recorded for the Pt/*m*-ZrO_2 sample after the first reaction cycle (20 h), whereas the Pt/*t*-ZrO_2 dropped only ~25% from its initial value. It evidences that a significant loss of metal dispersion occurs during the reaction and it is much likely related to sintering. Furthermore, dispersion seems to keep further declining during the second cycle and again the decrease is more significant for Pt/*m*-ZrO_2. This trend in dispersion diminishment is quite consistent with the deactivation pattern observed for these samples and supports the suggestion that metal sintering plays a quite important role in deactivation. A similar conclusion has already been related in the literature for Pt/TiO_2 [13].

Putting together all these findings, it can be concluded that the deactivation of ZrO_2-supported WGS catalysts can be associated with the drastic changes in metal dispersion during reaction. This fashion was identified over both polymorphic samples presented in this work. Therefore, new approaches should be taken into consideration to design an active, stable and cost-effective WGS catalyst to operate under real WGS reaction conditions.

4. Conclusion

It was found that zirconia polymorphism determines the catalyst activity and the monoclinic structure renders a more active system. This behavior is most likely due to the presence of hydroxyl surface groups, which have been claimed to be involved in the formation of important reaction intermediates.

WGS deactivation over the polymorphic catalysts is first and foremost associated with the decrease of platinum dispersion on time on stream.

Acknowledgments

The support from CNPq is acknowledged. E.M.A. thanks the grant provided by PCI/CNPq (181.722/09-7).

References

[1] C.H. Bartholomew, R.J. Farrauto, Fundamentals of Industrial Catalytic Processes, 2nd ed., Wiley-Interscience, 2006, p. 909.
[2] A.M. Duarte de Farias, D. Nguyen-Thanh, M.A. Fraga, Appl. Catal. B 93 (2010) 250.
[3] A.M. Duarte de Farias, A.P.M.G. Barandas, R.F. Perez, M.A. Fraga, J. Power Sources 165 (2007) 854.
[4] D. Nguyen-Thanh, A.M. Duarte de Farias, M.A. Fraga, Catal. Today 138 (2008) 235.
[5] P. Panagiotopoulou, D.I. Kondarides, Catal. Today 112 (2006) 49.
[6] A. Sandoval, A. Gómez-Cortés, R. Zanella, G. Díaz, J.M. Saniger, J. Mol. Catal. A 278 (2007) 200.
[7] P. Panagiotopoulou, D.I. Kondarides, Catal. Today 127 (2007) 319.
[8] I.D. González, R.M. Navarro, W. Wen, N. Marinkovic, J.A. Rodriguéz, F. Rosa, J.L.G. Fierro, Catal. Today 149 (2010) 372.
[9] K.G. Azzam, I.V. Babich, K. Seshan, L. Lefferts, J. Catal. 251 (2007) 153.
[10] G. Jacobs, P.M. Patterson, U.M. Graham, A.C. Crawford, B.H. Davis, Int. J. Hydrogen Energy 30 (2005) 1265.
[11] T. Bunluesin, R.J. Gorte, G.W. Graham, Appl. Catal. B 15 (1998) 107.
[12] T. Shido, Y. Iwasawa, J. Catal. 141 (1993) 71.
[13] K.G. Azzam, I.V. Babich, K. Seshan, L. Lefferts, Appl. Catal. A 338 (2008) 66.
[14] J.M. Pigos, C.J. Brooks, G. Jacobs, B.H. Davis, Appl. Catal. B 328 (2007) 14.
[15] D. Tibiletti, F.C. Meuner, A. Goguet, D. Reid, R. Burch, M. Boaro, M. Vicario, A. Trovarelli, J. Catal. 244 (2006) 183.
[16] P.S. Querino, J.R.C. Bispo, M.C. Rangel, Catal. Today 107–108 (2005) 920.
[17] L.V. Mattos, F.B. Noronha, J. Power Sources 145 (2005) 10.
[18] A. Zecchina, C. Lamberti, S. Bordiga, Catal. Today 41 (1998) 169.
[19] P.O. Graf, D.J.M. de Vlieger, B.L. Mojit, L. Lefferts, J. Catal. 262 (2009) 181.
[20] E. Chenu, G. Jacobs, A.C. Crawford, R.A. Keogh, P.M. Patterson, D.E. Sparks, B.H. Davis, Appl. Catal. B 59 (2005) 45.
[21] G. Águila, S. Guerrero, P. Araya, Catal. Commun. 9 (2008) 2550.
[22] J. Li, J. Chen, W. Song, J. Li, W. Shen, Appl. Catal. A 334 (2008) 321.
[23] Y. Zhao, W. Li, M. Zhang, K. Tão, Catal. Commun. 3 (2002) 239.
[24] A.A. Phatak, N. Koryabkina, S. Rai, J.L. Ratts, W. Ruettinger, R.J. Farrauto, G.E. Blau, W.N. Delgass, F.H. Ribeiro, Catal. Today 123 (2007) 224.
[25] G. Germani, P. Alphonse, M. Courty, Y. Schuurman, C. Mirodatos, Catal. Today 110 (2005) 114.
[26] X. Liu, W. Ruettinger, X. Xu, R. Farrauto, Appl. Catal. B 56 (2005) 69.
[27] S. Hilaire, X. Wang, T. Luo, R.J. Gorte, J. Wagner, Appl. Catal. A 215 (2001) 271.
[28] J.M. Zalc, V. Sokolovskii, D.G. Loffler, J. Catal. 206 (2002) 169.
[29] A. Gayen, M. Boaro, C. de Leitenburg, J. Llorca, A. Trovarelli, J. Catal. 270 (2010) 285.
[30] M.A. Fraga, E. Jordão, M.J. Mendes, M.M.A. Freitas, J.L. Faria, J.L. Figueiredo, J. Catal. 209 (2002) 355.
[31] F.B. Passos, M. Schmal, R. Fréty, Catal. Lett. 29 (1994) 109.
[32] F.B. Passos, E.R. Oliveira, L.V. Mattos, F.B. Noronha, Catal. Today 101 (2005) 23.
[33] J. Barbier, E. Churin, P. Marecot, J.C. Menezo, Appl. Catal. 36 (1988) 277.
[34] A.M. Silva, A.M. Duarte de Farias, L.O.O. Costa, A.P.M.G. Barandas, L.V. Mattos, M.A. Fraga, F.B. Noronha, Appl. Catal. A 334 (2008) 179.
[35] K.T. Jung, A.T. Bell, J. Mol. Catal. A 163 (2000) 27.
[36] G. Mestl, H. Knözinger, in: G. Ertl, H. Knözinger, J. Weitkamp (Eds.), Handbook of Heterogeneous Catalysis, vol. 2, Wiley, New York, 1997, p. 539.
[37] J.S. Cruz, M.A. Fraga, S. Braun, L.G. Appel, Appl. Surf. Sci. 253 (2007) 3160.
[38] G. Busca, J. Lamotte, J.C. Lavalley, V. Lorenzelli, J. Am. Chem. Soc. 109 (1987) 5197.
[39] G. Cerrato, S. Bordiga, S. Barbera, C. Morterra, Surf. Sci. 50 (1997) 377.
[40] A.O. Menezes, M.T. Rodrigues, A. Zimmaro, L.E.P. Borges, M.A. Fraga, Renew. Energy 36 (2011) 595.
[41] A.O. Menezes, P.S. Silva, E.P. Hernandez, L.E.P. Borges, M.A. Fraga, Langmuir 26 (2010) 3382.
[42] P. Panagiotopoulou, D.I. Kondarides, J. Catal. 260 (2008) 141.
[43] M. Boaro, M. Vicario, J. Llorca, C. Leitenburg, G. Dolcetti, A. Trovarelli, Appl. Catal. B 88 (2009) 272.
[44] A. Egbebi, V. Schwartz, S.H. Overbury, J.J. Spivey, Catal. Today 149 (2010) 91.
[45] Z.Y. Ma, C. Yang, W. Wei, W.H. Li, Y.H. Sun, J. Mol. Catal. A 231 (2005) 75.
[46] S.T. Korhonen, M. Calatayud, A.O.I. Krause, J. Phys. Chem. C 112 (2008) 16096.
[47] A. Gupta, M.S. Hegde, Appl. Catal. B 99 (2010) 279.
[48] J.A. Wang, A. Cuan, J. Salamones, N. Nava, S. Castillo, M. Moran-Pineda, F. Rojas, Appl. Surf. Sci. 230 (2004) 94.